

First-principles study of the adsorption of CO on TiO₂(110)

Zongxian Yang and Ruqian Wu*

Department of Physics, California State University, Northridge, California 91330-8268

Qiming Zhang

Department of Physics, The University of Texas at Arlington, Arlington, Texas 76019-0059

D. W. Goodman

Department of Chemistry, Texas A&M University, College Station, Texas 77843-3255

(Received 23 May 2000; published 9 January 2001)

The adsorption of CO on TiO₂(110) is investigated using the full-potential linearized-augmented-plane-wave method. The equilibrium structures of the clean and adsorbed TiO₂(110) surfaces are optimized through total-energy and atomic force calculations. Two geometries of CO absorption, namely, OC-Ti and CO-Ti, were considered. It is found that the former orientation is preferred. The calculated adsorption energy and redshift of the CO stretch frequency based on the local-density approximation are 0.79 eV/molecule and 23 cm⁻¹, respectively. The gradient corrections reduce the CO-TiO₂ binding energy to 0.25 eV/molecule. CO interacts with the TiO₂(110) substrate mainly via its 5σ state. Significant charge redistribution is involved in the CO/TiO₂(110) interaction, which changes the Coulomb potential and subsequently causes large shifts in the core and valence states of the CO adsorbate.

DOI: 10.1103/PhysRevB.63.045419

PACS number(s): 68.43.Mn

I. INTRODUCTION

Rutile TiO₂(110), the most thermodynamically stable TiO₂ surface, has been the focus of many experimental and theoretical studies because of the technological importance of titania in photocatalysts, chemical sensors, and heterogeneous catalysts.^{1,2} The Au/TiO₂ system, for example, was shown to exhibit properties suitable for application in chemical gas sensors and catalysts for room temperature CO oxidation.^{3–5} The authors of Refs. 6–9 found that CO oxidation on Au/TiO₂(110) is structure sensitive, and proposed that the unusual activity of the Au is likely due to quantum size effects in the highly dispersed Au clusters.

The nature of the bonding of CO to TiO₂(110) surfaces is a key to understanding CO oxidation reactions on titania and related catalysts [e.g., Au/TiO₂(110)]. Potential-energy surfaces and binding energies are essential to elucidate the nature of the catalytic active site as well as catalytic reactivity and selectivity. Experiments have shown that CO binds weakly to TiO₂. Infrared-absorption-spectroscopy studies¹⁰ found two states of CO on TiO₂ with stretch frequencies at 2115 and 2185 cm⁻¹, which correspond to a 28-cm⁻¹ redshift and a 42-cm⁻¹ blueshift, respectively, compared to that for the gas-phase CO (2143 cm⁻¹).¹¹ Earlier measurements for CO adsorption on polycrystalline rutile gave two bands at 2186 and 2206 cm⁻¹, corresponding to blueshifts of about 40–60 cm⁻¹.^{12–14} The adsorption energy (E_{ad}) of CO/TiO₂ was also measured by several groups with quite different values, ranging from ~0.4 eV (Ref. 15) in a more recent studies using thermal desorption spectroscopy, to 0.47–0.52 eV (Ref. 16) and 0.8 eV in other studies.¹⁷

Theoretical calculations found that CO adsorbs perpendicularly on the fivefold Ti sites of TiO₂(110), with the C end heading down. The optimized interatomic distance $d_{C,Ti}$ are in a narrow range 2.33–2.5 Å. The calculated CO adsorp-

tion energies (E_{ad}) on TiO₂(110), however, scatter widely, and strongly depend on the computational details. Using a cluster model and a molecular orbital method, Kobayashi and Yamaguchi¹⁸ obtained 0.73 eV for E_{ad} . Using a two-dimensional TiO₂ chains to model the TiO₂ surfaces and the periodic Hartree-Fock crystalline orbital method, Fahmi and Minot¹⁹ gave a range for E_{ad} , 0.5–0.9 eV, depending the model and the basis set. Using a cluster model embedded in electrostatic multiples obtained from slab calculations, Reinhardt *et al.*²⁰ found that, depending on the choice of exchange-correlation functions, the calculated binding energies vary from 0.26 to 0.52 eV. The authors of Ref. 21 through both cluster and slab model calculations, reported a binding energy of 0.7–0.8 eV for CO/TiO₂(110) at low coverage. Their results of CO stretch frequency shifts, 130–140 cm⁻¹, are too high compared to the experimental data.^{10,12–14}

Most of these theoretical studies^{18,19,21} were carried on the unrelaxed TiO₂(110) surface. It is known^{22–24} that strong surface relaxation and reconstruction occur at the TiO₂(110) surface, and these structural alternations are expected to affect the binding of TiO₂(110) to an adsorbate.²⁰ Furthermore, these calculations might be affected by various approximations such as cluster size, basis set superposition error,²⁰ etc. Studies using more accurate methods and models are clearly needed to provide a more reliable picture of CO bonding on titania.

In this study, the highly precise full-potential linearized-augmented-plane-wave (FLAPW) method²⁵ is used to study the adsorption of CO on the TiO₂(110) surface. The normal adsorption modes with either the C (denoted as OC-Ti) or O (denoted as CO-Ti) atom heading toward the fivefold surface Ti atom are considered. As found in previous calculations, CO “prefers” the OC-Ti mode. Using the local-density approximation (LDA),²⁶ the calculated adsorption energy and the redshift of the CO stretch frequency are 0.79 eV/

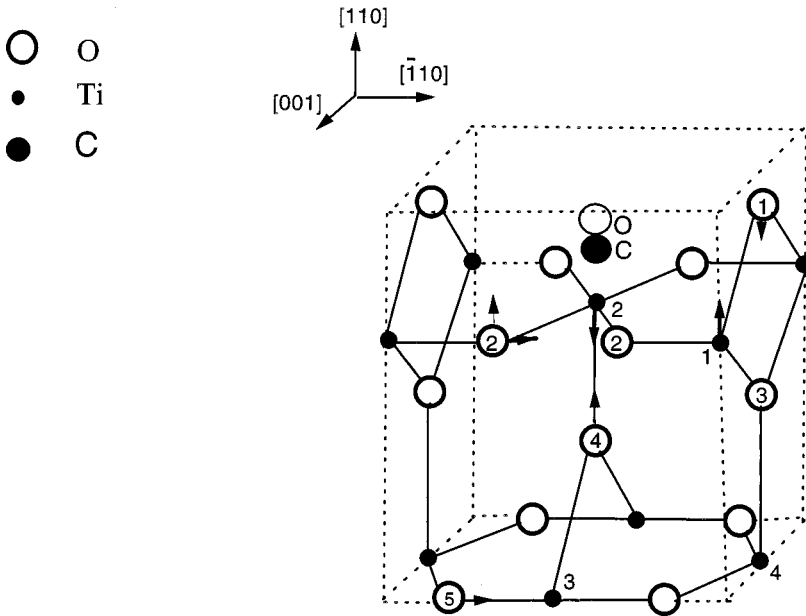


FIG. 1. The schematic geometry of the bulk-terminated $\text{TiO}_2(110)-(1 \times 1)$ (only the upper half of the three-layer slab is drawn). Small solid circles represent Ti, and large open circles are for O. The CO is placed on the atop site above Ti(2), with its C end toward the substrate.

molecule and 23 cm^{-1} , respectively. The equilibrium bond lengths are $d_{\text{C-Ti}} = 2.37 \text{ \AA}$ and $d_{\text{C-O}} = 1.129 \text{ \AA}$. In contrast, the generalized gradient approximation (GGA)²⁷ reduces the CO adsorption energy to 0.25 eV.

II. MODEL AND COMPUTATIONAL METHOD

The film version of the FLAPW method²⁵ uses a single slab model to simulate surfaces, and has no shape approximation for charge, potential, and wave functions in the muffin-tin, interstitial, and vacuum regions. The formalisms of Hedin and Lundqvist (LDA)²⁶ and of Ref. 27 (GGA)²⁷ were used to describe the exchange-correlation potential and energy.

In the muffin-tin region, spherical harmonics with a maximum angular momentum of 8 are used to expand the charge, potential, and wave functions. In the interstitial region, plane waves with energy cutoffs of 324 Ry (for the charge and potential) and 30 Ry (for the variational bases, corresponding to a plane wave basis set of 6900 APW's/cell) were employed. Ti- $3p3d4s$, C- $2s2p$, and C- $2s2p$ states were treated as valence states. For such a large basis set, we used the parallelized version of our FLAPW code with 32 or 64 Cray-T3E processors.

The equilibrium structures were determined using total-energy and atomic force approaches,²⁸ with a criterion that requires the force on each atom to be less than 2×10^{-3} Hartree/a.u. 16 k points in the irreducible part of the two-dimensional Brillouin zone were used for the integrals in the reciprocal space. Self-consistency is assumed when the root-mean-square distances between the input and output charge densities become less than 1.0×10^{-6} electrons/a.u.³

III. RESULTS AND DISCUSSIONS

Our recent studies²⁴ for bulk TiO_2 showed that the lattice constants calculated with the LDA ($a = 4.594 \text{ \AA}$, $c = 2.952 \text{ \AA}$) agree with the experimental values.²⁹ In addition,

the LDA bulk modulus ($B = 228 \text{ GPa}$) is also very close to the observed value (239 GPa).³⁰ By contrast, the GGA was found to overestimate the lattice constant of bulk TiO_2 by 2%. The LDA thus appears to be more suitable for simulations of the $\text{TiO}_2(110)$ surface, especially for structural optimization.

The $\text{TiO}_2(110)$ substrate used here is modeled by a three-layer slab shown in Fig. 1 (only the upper half of the slab is shown). The atoms in the model are fully relaxed according to their atomic forces. Ramamoorthy and co-workers²³ showed that this thickness is sufficient to obtain accurate results of structural relaxation and surface energy. As reported previously,²²⁻²⁴ the calculated atomic displacements from their ideal positions occur mainly along the surface normal with the fivefold Ti [denoted as Ti(2)] and the sixfold Ti [denoted as Ti(1)] moving inward and outward by 0.15 and 0.13 \AA , respectively. The bridging oxygen [denoted as O(1)] and the in-plane oxygen [denoted as O(2)] move inward and outward by ~ 0.06 and 0.13 \AA , respectively. The O(2) and O(5) atoms also relax laterally by 0.06 and 0.05 \AA , respectively, along the $[\bar{1}10]$ direction as indicated in Fig. 1. The relaxed $\text{TiO}_2(110)$ surface is puckered, a result that agrees well with earlier theoretical results for a five-layer slab²³ as well as with x-ray diffraction data.²²

Properties of a free CO molecule are simulated by using a two-dimensional square lattice of CO with a varying lattice constant. Test calculations showed that the CO-CO interaction is negligible when the lattice constant becomes larger than 4.0 \AA ; a square lattice with $a = 5.3 \text{ \AA}$ is used for final results. The calculated total energies and atomic forces for different CO bond lengths with the LDA indicate that CO has an equilibrium bond length of 1.126 \AA and a binding energy of 12.5 eV. The stretch frequency of CO is 2143 cm^{-1} . By contrast, the GGA yields a larger C-O bond length (1.133 \AA), a smaller binding energy of 11.9 eV, and a smaller vibration frequency (2106 cm^{-1}). Comparing with the experimental data for free CO [stretch frequency: 2143

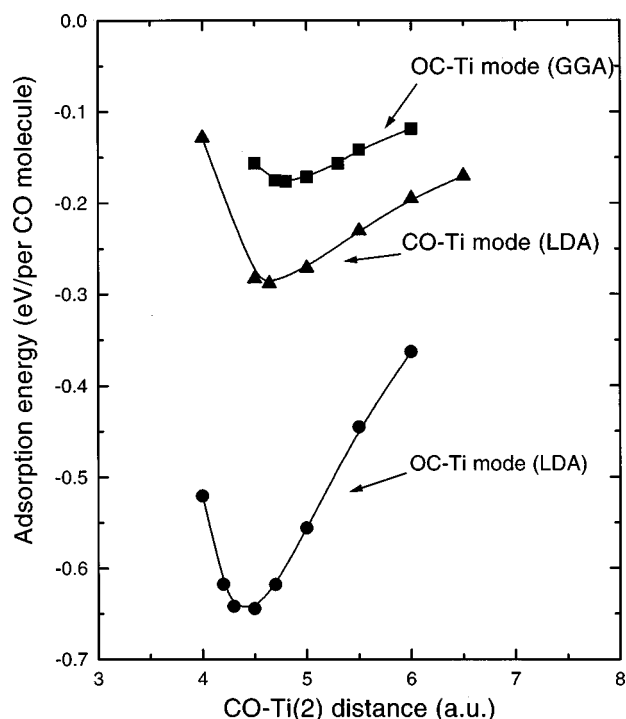


FIG. 2. The adsorption energies of CO/TiO₂(110) vs the CO-Ti(2) distance ($d_{\text{C-Ti}}$ for the OC-Ti mode or $d_{\text{C-Ti}}$ for the CO-Ti mode) with a fixed CO bond length ($d_{\text{C-O}}=2.14$ a.u.)

cm^{-1} (Ref. 11) and 2148 cm^{-1} (Ref. 20); binding energy: 11.24 eV (Ref. 31)]. The LDA appears to give a better frequency but a worse binding energy and bond length than the GGA for a free CO.

For the adsorption of CO on a TiO₂(110) surface, a pseudomorphic CO monolayer is placed on each side of the relaxed TiO₂(110) surface above the Ti(2) atom. To calculate the adsorption energy, the substrate geometry and the CO bond length (1.132 \AA) were fixed first. The adsorption energies of the CO/TiO₂(110) system [defined as $E_{\text{ad}} = \frac{1}{2}(E_{2\text{CO-TiO}_2} - E_{\text{TiO}_2} - E_{2\text{CO}})$, with $E_{2\text{CO-TiO}_2}$, E_{TiO_2} and $E_{2\text{CO}}$ representing the total energies of the adsorbed system for the clean TiO₂(110) surface and two pseudomorphic CO monolayers] are shown in Fig. 2 as a function of the CO-Ti distances ($d_{\text{C-Ti}}$ for the OC-Ti mode and $d_{\text{C-Ti}}$ for the CO-Ti mode). It is clearly shown that CO prefers the OC-Ti geometry, with an adsorption energy (LDA) of 0.64 eV per CO molecule and a bond length of $d_{\text{C-Ti}}=2.37 \text{ \AA}$. For the CO-Ti mode, the adsorption energy curve minimizes at a larger bond length $d_{\text{C-Ti}}=2.45 \text{ \AA}$, with a much smaller adsorption energy (0.29 eV per CO molecule). The large energy difference between the two geometries (0.35 eV per CO molecule) indicates the stability of the OC-Ti case. Using the GGA, the adsorption energy curve shown in Fig. 2 yields a larger C-Ti bond length (2.54 \AA), but a much smaller E_{ad} (0.18 eV/molecule). If a free CO molecule is used as the reference, the adsorption energies for the OC-Ti mode are enhanced to 0.79 eV (LDA) and 0.25 eV (GGA), respectively.

Our results for E_{ad} suggest that the GGA and LDA set a

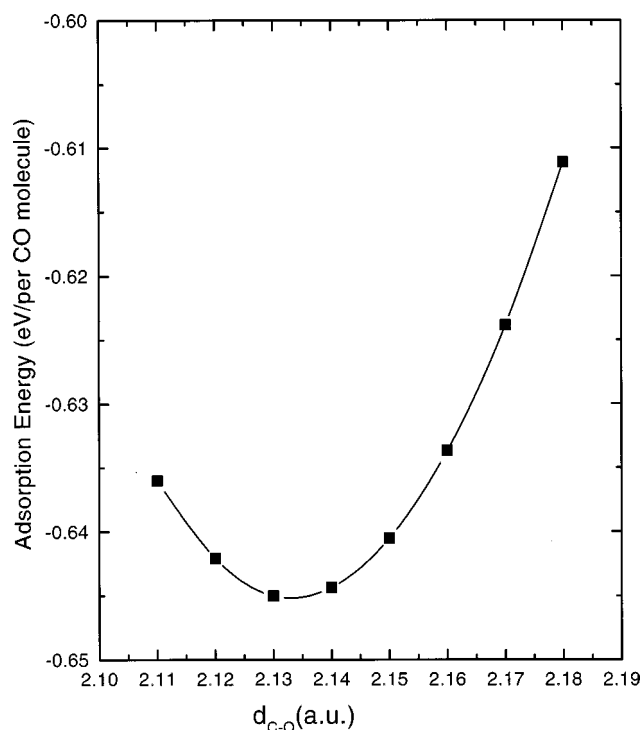


FIG. 3. The adsorption energies (LDA) of CO/TiO₂(110) vs the CO bond length ($d_{\text{C-O}}$), with a fixed C-Ti(2) distance ($d_{\text{C-Ti}}=4.47$ a.u.)

correct range for the experimental data available ($0.4\text{--}0.8 \text{ eV}$). A final conclusion about whether the LDA or the GGA is more appropriate for this system awaits more experimental results, with a minimum influence of surface defects to compare with. Nevertheless, as demonstrated in our previous studies, gradient corrections do not change charge-density profiles and the density of states appreciably. We focus on the LDA results for discussions of other properties below.

The CO bond length ($d_{\text{C-O}}$) is then allowed to relax with $d_{\text{C-Ti}}$ fixed at 2.37 \AA . The dependence of the total energy on $d_{\text{C-O}}$ is shown in Fig. 3. The optimized CO bond length is 1.129 \AA , only 0.003 \AA larger than that for free CO (1.126 \AA). The total-energy change due to the CO relaxation is only 0.001 eV , justifying the two-step treatment of the C-Ti and C-O relaxations. With a CO adsorbate, the forces on the substrate atoms remain small, and thus the adsorbate-induced surface relaxation and reconstruction on TiO₂(110) is negligible. This is consistent with the weak CO-surface bond in CO/TiO₂(110).

Using a model of two springs with elastic constants calculated from the LDA total-energy curves, the CO intermolecular and intramolecular stretch frequencies are 170 and 2120 cm^{-1} , respectively. The calculated CO stretch frequency corresponds to a redshift of 23 cm^{-1} compared to that for a free CO molecule (2143 cm^{-1}).¹¹ Both values agree with the experimentally determined values (2115 and 28 cm^{-1}) for one of the CO adsorption states.¹⁰ The other higher stretch frequencies observed by experiments [2185 cm^{-1} (Ref. 16) or 2206 cm^{-1} (Refs. 12–14)] are believed to correspond to CO adsorbed on other sites, or caused due to some other reason such as surface defects.

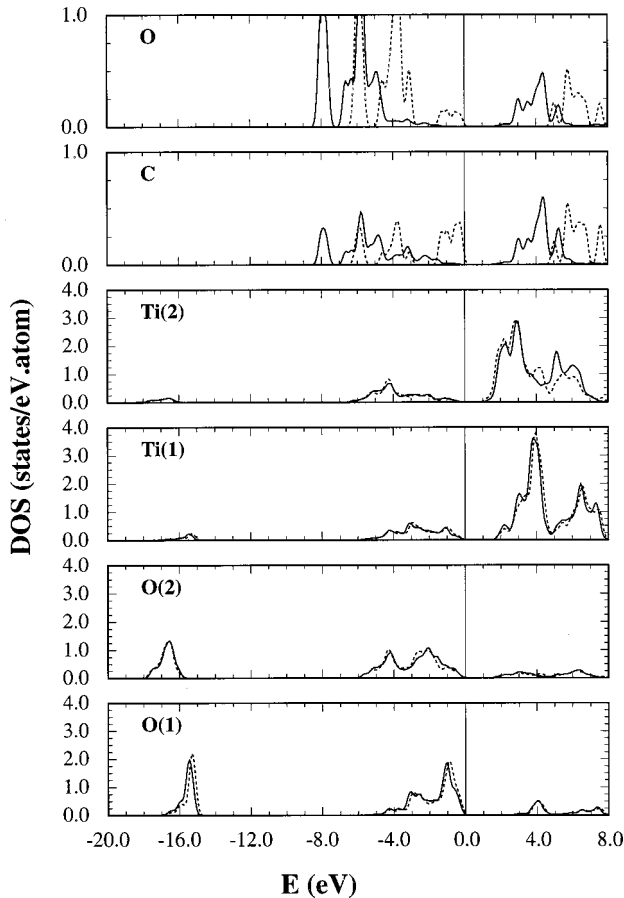


FIG. 4. The local density of states (LDOS) for CO/TiO₂(110) (solid lines), and that for the reference systems [a free pseudomorphic CO monolayer and a clean TiO₂(110) surface] (dotted lines).

The local density of states (LDOS) for the adsorbed system and the reference systems [i.e., the pseudomorphic free CO monolayer and the clean TiO₂(110)] are shown in Fig. 4 [reference systems are dashed; CO/TiO₂(110) are solid]. For the free CO ML, the 4σ , 1π , and 5σ peaks in the DOS curves are well separated. The computed ($4\sigma-1\pi$) separation and ($1\pi-5\sigma$) separation are about 2.0 and 3.0 eV, respectively, in good agreement with the experiment values (2.7 and 2.9 eV, respectively).²¹ When CO is adsorbed on TiO₂(110), the 4σ , 1π , and $2\pi^*$ states undergo a large energy shift (stabilized by ~ 2 eV), while the ($4\sigma-1\pi$) separation remains unchanged. The CO 5σ peak undergoes an even larger energy shift, which is significantly broadened and lowered and merged with the 1π peak. This phenomenon was also demonstrated in Ref. 21. Clearly, CO interacts with the substrate mainly via its 5σ state, leading to stabilization due to charge transfer [cf. panel (d) in Fig. 5 and panel (b) in Fig. 6]. On the other hand, only very slight changes are induced in the LDOS curves of the substrate atoms in the occupied region, showing the weakness of the CO/TiO₂(110) interaction.

To further investigate the bonding mechanism for the adsorption of CO on TiO₂(110), the charge densities are presented in Fig. 5 for the free CO monolayer [in panel (a)], the clean TiO₂(110) surface [in panel (b)] and the CO/TiO₂(110)

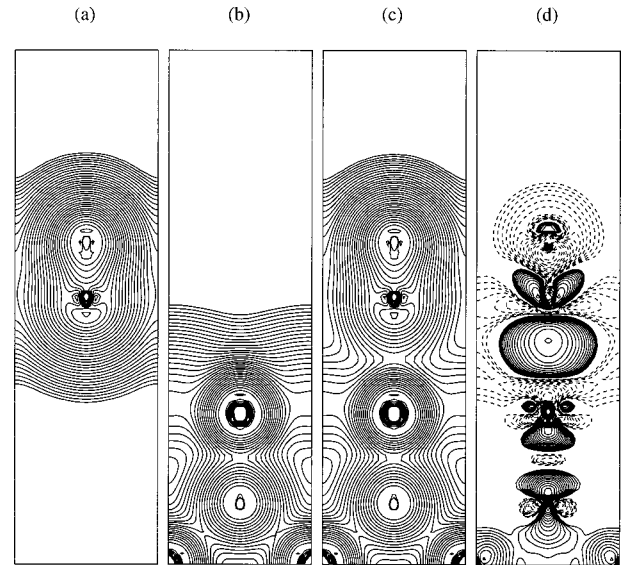


FIG. 5. The calculated valence charge densities for (a) the CO monolayer, (b) the TiO₂(110) clean surface, (c) the CO/TiO₂(110) system, and (d) the charge-density difference obtained by subtracting the superposition of the charge densities of the CO monolayer and TiO₂(110) from that of CO/TiO₂(110). Contours shown in the vertical ($\bar{1}10$) plane start from 5×10^{-4} e/a.u.³ in panels (a)–(c) and from $\pm 5 \times 10^{-4}$ e/a.u.³ in panel (d), and increase successively by a factor of $10^{0.1}$. Dashed lines in panel (d) indicate negative differences.

system [in panel (c)]. As expected, contours for the TiO₂(110) clean surface show strong corrugation in the vacuum region with a minimum on top of the Ti(2) atom because of the inward relaxation of the Ti(2) atoms and the ionic bonding of TiO₂ (electron transfer from Ti to O). The charge density in the region between CO adsorbates is smaller than 8×10^{-3} e/a.u.³, which indicates the weakness of the interaction among CO adsorbates. In Fig. 5(d) the difference in charge density obtained by subtracting the superposition of charge densities in panels (a) and (b) from those in panel (c) is plotted. Noticeable electron accumulation in the region between the carbon and Ti(2) sites suggests hybridization of the CO- 5σ and the Ti(2)- d states. This is very similar to that found for the CO/MgO(001) system,^{32,33} but quite dissimilar to that seen for the CO/Au systems.³⁴ CO appears to interact with oxides primarily via the 5σ state, whereas virtually all the CO states (including the $2\pi^*$ state) are involved in the bonding of CO with Au, even though the values of E_{ad} are very similar for these two adsorption systems.

The planar average charge density (PACD) from the center layer to the vacuum along the surface normal is shown in Fig. 6(a). The PACD difference [obtained by subtracting the superposition of the PACD's of CO monolayer and TiO₂(110) from that of CO/TiO₂(110)] due to the adsorption of CO is shown in Fig. 6(b). The features in panel (a) indicate positions of different atomic layers along the $[110]$ direction. As denoted in panel (a), the pronounced peaks correspond to charge densities of the mixed layers of Ti and O, while the minor peaks correspond to charge densities of

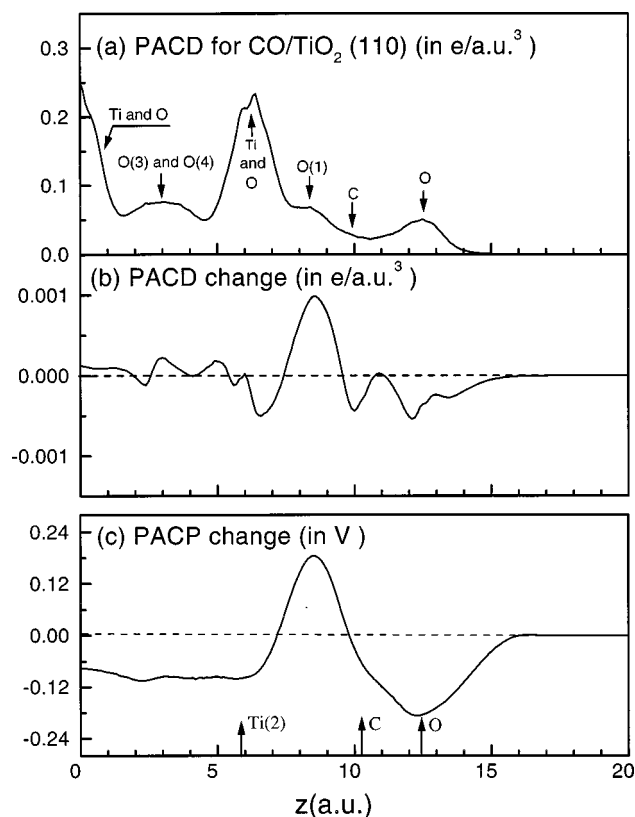


FIG. 6. (a) The planar average charge density (PACD) along the surface normal for the CO/TiO₂(110) system. (b) The PACD difference between the adsorbed system and the reference systems. (c) The planar average Coulomb potential (PACP) difference.

O-only layers in the substrate and to C and O layers in the CO molecule. The PACD change shown in panel (b) indicates that electron depletion from both the CO molecule and the surface Ti(2) sites occurs with accumulation in the region between them. Correspondingly, as shown in panel (c), the Coulomb potential increases in the interfacial area between CO and TiO₂(110), and decreases both in the substrate and in the CO layer. This results in energy shifts of the CO core and valence states. The CO valence states are stabilized by

~2 eV. The calculated binding energies of the core states of CO(C-1s_{1/2}, O-1s_{1/2}) in CO/TiO₂(110) are stabilized by 2.40 and 2.24 eV, respectively, compared to the corresponding values for a free, pseudomorphic CO monolayer. These binding-energy shifts are very close to those for the valence states of CO, consistent with a common origin for each, namely, charge polarization in the interfacial region. For the substrate atoms, the core-level binding energies of Ti(2)-2p_{3/2} and O(1)-1s_{1/2} are also stabilized slightly by 0.17 and 0.07 eV, respectively, compared to those found for the clean TiO₂(110) surface.

IV. SUMMARY

The bonding mechanism and binding energy of CO on TiO₂(110) were investigated using the FLAPW method. Calculations show that the OC-Ti adsorption mode is preferred. With the LDA, the calculated adsorption energy and the redshift of the CO stretch frequency are 0.79-eV/molecule and 28 cm⁻¹, respectively, showing that CO binds weakly to the TiO₂(110) surface, in agreement with experiment. Gradient corrections (GGA) reduce the CO-TiO₂ binding energy to 0.25 eV/molecule. Our results for E_{ad} suggest that the GGA and LDA set a correct range for the experimental data available (0.4–0.8 eV). A final conclusion about whether the LDA or GGA is more appropriate for this system awaits more experimental results with minimal influence from surface defects to compare with. CO interacts with the TiO₂(110) substrate mainly via its 5σ state. A significant charge redistribution is involved in the bonding of CO to TiO₂(110), which results in large energy shifts for the CO core and valence states (4σ, 1π, and 2π*).

ACKNOWLEDGMENTS

This work was supported by the U.S. Department of Energy, Office of Basic Energy Sciences, Division of Chemical Sciences [Grant No. DE-FG03-99ER14948 (Z. Y. and R. W.) and Grant No. DE-FG03-95ER14511 (D. W. G.)], and by computing time from NERSC. The Parson's foundation is also gratefully acknowledged for providing the funding to upgrade the computer facilities at CSUN.

*Corresponding author: ruqian.wu@csun.edu

¹R. J. Lad, *Surf. Rev. Lett.* **12**, 109 (1995).

²A. M. Azad, S. A. Akbar, S. G. Mhaisalkar, L. D. Birkefeld, and K. S. Goto, *J. Electrochem. Soc.* **139**, 3690 (1992).

³T. Kobayashi, M. Haruta, H. Sano, and M. Nakane, *Sens. Actuators* **13**, 39 (1988).

⁴S. D. Lin, M. Bollinger, and M. A. Vannice, *Catal. Lett.* **17**, 245 (1993).

⁵S. Lin and M. A. Vannice, *Catal. Lett.* **10**, 47 (1991).

⁶M. Valden, X. Lai, and D. W. Goodman, *Science* **281**, 1647 (1998).

⁷M. Valden, S. Pak, X. Lai, and D. W. Goodman, *Catal. Lett.* **56**, 7 (1996).

⁸D. R. Rainer and D. W. Goodman, *J. Mol. Catal. A: Chemical* **131**, 259 (1998).

⁹X. Lai, T. P. St. Clair, M. Valden, and D. W. Goodman, *Prog.*

Surf. Sci. **59**, 25 (1998).

¹⁰K. Tanaka and J. M. White, *J. Phys. Chem.* **86**, 4708 (1982); *J. Catal.* **79**, 81 (1983).

¹¹S. C. Street, C. Xu, and D. W. Goodman, *Annu. Rev. Phys. Chem.* **48**, 43 (1997).

¹²K. Hadjiivanov, A. Davydov, and D. Klissursky, *Kinet. Katal.* **29**, 161 (1988).

¹³G. Busca, A. Saussey, D. Saur, J. C. Lavalley, and V. Lorenzelli, *Appl. Catal.* **14**, 245 (1985).

¹⁴C. Morterra, E. Garrone, V. Bolis, and B. Fubini, *Spectrochim. Acta, Part A* **43**, 1577 (1987).

¹⁵Amy Linsebigler, Guangquan Lu, and John T. Yates, Jr., *J. Chem. Phys.* **103**, 9438 (1995).

¹⁶G. B. Raupp and J. A. Dumestic, *J. Phys. Chem.* **89**, 5240 (1985).

¹⁷W. Göpel, G. Rocker, and R. Feierabend, *Phys. Rev. B* **28**, 3427 (1983).

- ¹⁸H. Kobayashi and M. Yamaguchi, *Surf. Sci.* **214**, 466 (1989).
- ¹⁹A. Fahmi and C. Minot, *J. Organomet. Chem.* **478**, 67 (1994).
- ²⁰P. Reinhardt, M. Causà, C. M. Marian, and B. A. Heß, *Phys. Rev. B* **54**, 14 812 (1996).
- ²¹G. Pacchioni, A. M. Ferrari, and P. S. Bagus, *Surf. Sci.* **350**, 159 (1996).
- ²²G. Charlton, P. B. Howes, C. L. Nicklin, P. Steadman, J. S. G. Taylor, C. A. Murny, S. P. Harte, J. Merce, R. McGrath, D. Norma, T. S. Turner, and G. Thornton, *Phys. Rev. Lett.* **78**, 495 (1997).
- ²³M. Ramamoorthy, D. Vanderbilt, and R. D. King-Smith, *Phys. Rev. B* **49**, 16 721 (1994); M. Ramamoorthy, R. D. King-Smith, and D. Vanderbilt, *ibid.* **49**, 7709 (1994).
- ²⁴Zongxian Yang, Ruqian Wu, and D. W. Goodman, *Phys. Rev. B* **61**, 14 066 (2000).
- ²⁵E. Wimmer, H. Krakauer, M. Weinert, and A. J. Freeman, *Phys. Rev. B* **24**, 864 (1981); M. Weinert, E. Wimmer, and A. J. Freeman, *ibid.* **26**, 4571 (1982), and references therein.
- ²⁶L. Hedin and S. Lundqvist, *J. Phys. C* **33**, 373 (1972).
- ²⁷J. P. Perdew, K. Burke, and M. Ernzerhof, *Phys. Rev. Lett.* **77**, 3865 (1996).
- ²⁸J. M. Soler and A. R. Williams, *Phys. Rev. B* **40**, 1560 (1989); R. Yu, D. Singh, and H. Krakauer, *ibid.* **43**, 6411 (1992).
- ²⁹P. Vinet, J. Ferrante, J. R. Smith, and J. H. Hose, *J. Phys.: Condens. Matter* **19**, L467 (1986).
- ³⁰*CRC Handbook of Chemistry and Physics*, 77th ed., edited by D. Lide (CRC Press, Boca Raton, FL, 1997).
- ³¹B. Hammer, L. B. Hansen, and J. K. Nørskov, *Phys. Rev. B* **59**, 7413 (1999).
- ³²Lujun Chen, Ruqian Wu, N. Kioussis, and Qiming Zhang, *Chem. Phys. Lett.* **290**, 255 (1998).
- ³³Ruqian Wu and Qiming Zhang, *Chem. Phys. Lett.* **306**, 205 (1999).
- ³⁴Ruqian Wu (unpublished).